

# A transformation $I_2 \cdot I^- \cdot I_2 \leftrightarrow I_3^- \cdot I_2$ in the pentaiodide complex $(\alpha\text{-Cyclodextrin})_2 \cdot Cd_{0.5} \cdot I_5 \cdot 26H_2O$ , detected via dielectric and Raman spectroscopy

Vasileios G. Charalampopoulos, John C. Papaioannou\*, Konstantinos E. Tampouris

Department of Chemistry, Laboratory of Physical Chemistry, National and Kapodistrian University of Athens P.O. BOX 64004, 157 10 Zografou, Athens–Greece

Received 14 July 2006; received in revised form 23 January 2007; accepted 20 February 2007

## Abstract

The ac-conductivity and the phase shift of the polycrystalline complex  $(\alpha\text{-CD})_2 \cdot Cd_{0.5} \cdot I_5 \cdot 26H_2O$  ( $\alpha\text{-CD} = \alpha\text{-Cyclodextrin}$ ) have been investigated over the frequency and temperature ranges of 0–100 kHz and 240–425 K. A Raman spectroscopy study is also accomplished in the temperature ranges of (i) 153–293 K and (ii) 303–383 K. From 276.2 up to 335.6 K – where all the water molecules of the crystal lattice exist – the transformation  $(H_2O)_{\text{tightlybound}} \rightarrow (H_2O)_{\text{easily movable}}$  takes place, resulting in the linear increment of the ac-conductivity in the  $\ln \sigma$  vs.  $1/T$  plot with activation energy  $E_a = 0.51$  eV. In the range of 335.6–377.0 K a second linear part with  $E_a = 0.67$  eV is observed attributed to the contribution of  $Cd^{2+}$  ions via the water-net. At  $T > 377.0$  K, the abrupt decrease of the ac-conductivity up to 401.6 K is due to the removal of all the water molecules from the lattice. The phase shift presents a topical minimum at 404.3 K directly related to an order–disorder transition of the  $I^-$  ions in some pentaiodide units and an abrupt decrease at  $T > 412.9$  K due to the sublimation of iodine molecules. The Raman spectra at room temperature present two bands at 160 and 168  $cm^{-1}$  indicating the coexistence of two kinds of pentaiodide units  $I_2 \cdot I^- \cdot I_2$  and  $I_3^- \cdot I_2 \leftrightarrow I_2 \cdot I_3^-$ , respectively. Because of the inverse transformation  $(I_3^- \cdot I_2 \leftrightarrow I_2 \cdot I_3^-) \leftrightarrow (I_2 \cdot I^- \cdot I_2)$  the band at 168  $cm^{-1}$  disappears as the temperature decreases whereas the band at 160  $cm^{-1}$  disappears during the heating process. The X-ray powder diffraction and the Rietveld analysis revealed a tetragonal crystal form with space group  $P4_22_12$  and lattice parameters that are in good agreement with the theoretical values.  
© 2007 Elsevier B.V. All rights reserved.

**Keywords:** Dielectric properties; Raman spectra;  $\alpha$ -Cyclodextrin complex; Pentaiodide ions; Rietveld refinement

## 1. Introduction

The aqueous solutions of  $\alpha$ - and  $\beta$ -cyclodextrins ( $\alpha$ -CDs,  $\beta$ -CDs) with metal iodides ( $M^+I^-$ ) and iodine can form inclusion complexes. The  $\alpha$ - and  $\beta$ -CD molecules are stacked in a head to head arrangement producing dimers in whose tubular cavities polyiodide chains are developed. All the  $\beta$ -CD complexes are crystallized in monoclinic  $P2_1$  form for different metals and the polyiodide chains consist of non interactive heptaoidide ions  $I_7^-$  shaped into a Z-like structure  $(I_2 \cdot I_3^- \cdot I_2)$  [1]. The atoms of the two  $I_2$  units within the  $\beta$ -CD cavities, are disordered in positions with main (0.82, 0.70) and minor (0.15, 0.14) occupancies whereas the atoms of the central  $I_3^-$  unit are in

positions with full occupancy. The  $\alpha$ -CD complexes are crystallized in four different crystal forms (triclinic, tetragonal, pseudohexagonal, hexagonal) depending on the counterion's nature and the polyiodide chains consist of weakly interactive linear pentaoidide ions  $I_5^-$  ( $I_2 \cdot I^- \cdot I_2$  or  $I_3^- \cdot I_2$  type). The atoms of the two  $I_2$  units within the  $\alpha$ -CD cavities are well-ordered (full occupancy) whereas the central  $I^-$  ion is disordered in various occupancy ratios [2].

Specifically, the single crystal X-ray analysis [2,3] of the  $(\alpha\text{-CD})_2 \cdot Cd_{0.5} \cdot I_5 \cdot 27H_2O$  complex (named  $\alpha$ -Cd) has shown that it crystallizes in the tetragonal crystal form with space group  $P4_22_12$  and the occupancy ratio of the central  $I^-$  ion in the linear  $I_5^-$  units is 50/50 ( $I_2 \cdot I^- \cdot I_2$  type) at room temperature (Fig. 1). The separation distance between the neighboring  $I_5^-$  units is 3.32 Å, indicating electron delocalization, whereas the 27 water molecules are located outside the  $\alpha$ -CD stacks. The  $Cd^{2+}$

\* Corresponding author. Fax: +3210 7274752.

E-mail address: [jpapaioannou@chem.uoa.gr](mailto:jpapaioannou@chem.uoa.gr) (J.C. Papaioannou).

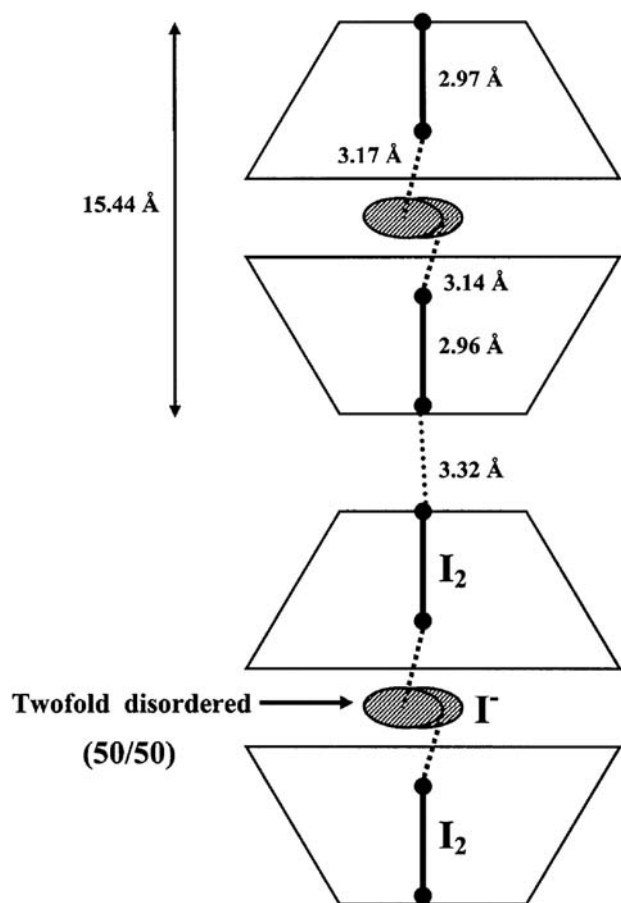


Fig. 1. Geometry of the polyiodide chain in  $(\alpha\text{-CD})_2\cdot\text{Cd}_{0.5}\cdot\text{I}_5\cdot 27\text{H}_2\text{O}$  according to Ref. [2]. The central  $\Gamma$  ions in the pentaiodides are twofold disordered.

cations are also twofold disordered ( $\text{Cd}(0.5)$ ,  $\text{Cd}^*(0.5)$  per dimer) with both sites located on the twofold axes //c and surrounded by hydration shells without direct contact to the  $\alpha\text{-CD}$  hydroxyls. The site Cd is octahedrally coordinated by water molecules while the site  $\text{Cd}^*$  is surrounded irregularly by 6 water molecules.

The temperature dependence of the dielectric constant ( $\epsilon'$ ,  $\epsilon''$ ) and the phase shift  $\varphi$  of the  $\alpha\text{-Cd}$  complex in the temperature range of 120–300 K [4] revealed: (i) the transformation of some normal hydrogen bonds to those of flip-flop type [5,6] and (ii) the existence of two kinds of water molecules, tightly bound and easily movable, since they do not occupy equivalent positions and have different surroundings. The same behaviour was observed for numerous  $\alpha$ - and  $\beta$ -CD polyiodide complexes [7–10] in the above temperature range, where all the water molecules of the crystal lattice exist.

At elevated temperatures the parameters  $\epsilon'$ ,  $\epsilon''$  lose their reliability due to the high conductivity values. In these cases the ac-conductivity ( $\sigma$ ) and the phase shift ( $\varphi$ ) can reveal all the different mechanisms of charge transport that take place in the sample (e.g. proton conduction, metallic movements, polyiodide interactions and dehydration process). These effects have been analyzed only for the  $\beta$ -CD complexes ( $\beta\text{-Ba}$ ,  $\beta\text{-Cd}$ ,  $\beta\text{-Li}$ ,  $\beta\text{-K}$  and  $\beta\text{-Cs}$ ) [7–9] whose dielectric investigation was

extended up to 420 K in combination with their Raman spectra and calorimetric measurements. It was found that the contribution of the water-net work to the ac-conductivity ( $\sigma$ ) was amplified by the movements of the metal ions. The temperature dependence of  $\sigma$  presented deviations (lower increasing rate) from the Arrhenius exponential behaviour  $\sigma = \sigma_0 \exp(-E_W/2k_B T)$  during the dehydration process and a rapid increase at approximately 403 K, due to the sublimation of iodine which shortens the neighboring  $\text{I}_7^-$  ions. Finally, all the above  $\beta$ -CD complexes showed a shift of the initial Raman band at  $179\text{ cm}^{-1}$  to the final value  $165\text{--}166\text{ cm}^{-1}$  during the heating process, indicating an order–disorder transformation of the  $\text{I}_2$  units.

The above correlation of dielectric measurements, Raman spectra and thermal analysis, provided sufficient information about the isomorphous  $\beta$ -CD hepta-iodide complexes and established a foundation for extending our studies to the polymorphous  $\alpha$ -CD penta-iodide inclusion complexes. These systems are expected to present discrete conduction properties due to the various penta-iodide formations and the different coordination schemes of the metal ions. Initially, we turn our attention to the tetragonal  $\alpha$ -Cd complex whose large spaces between the  $\alpha$ -CD stacks are enriched by a great amount of water molecules (27 charge carriers per dimer) and the disordered  $\text{Cd}^{2+}$  ions, revealing a direct relation between the metallic movements and the proton transport. We were also motivated by the Raman examination of the single crystal of  $\alpha$ -Cd by Mizuno et al. at room temperature [11]. The researchers observed two bands at  $107$  and  $161\text{ cm}^{-1}$  and ascribed them to the varied composition of disordered  $(\text{I}_3)_x$  and  $(\text{I}_5)_x$  chains, respectively. These results indicate a more complicated polyiodide structure than that described by Noltemeyer and Saenger [2].

Therefore, in the present work we investigate the ac-conductivity and the phase shift of  $\alpha$ -Cd over the frequency range of 0–100 kHz and the extended temperature range of 240–425 K, where the removal of the water molecules and polyiodide charge transfer interactions take place. Besides this, the Raman spectra are investigated in the temperature ranges of (i) 153–293 K and (ii) 303–383 K in order to explore the variations in the  $\text{I}_5^-$  units.

## 2. Experimental

$\alpha$ -Cyclodextrin, iodine and cadmium iodide were purchased from Fluka Chemica. 5.5 g of  $\alpha$ -CD was dissolved in 40 ml of distilled water at room temperature under stirring until the solution became almost saturated. Then 0.21 g cadmium iodide and 0.22 g solid iodine were added simultaneously to the solution and it was heated up to  $70\text{ }^\circ\text{C}$  for 20–25 min. The hot solution was transferred quickly through a folded filter to an empty beaker (100 ml) which was covered with Teflon and then immersed in a Dewar flask (500 ml) containing water at the same temperature. After 2 days, very fine thin needles of  $\alpha$ -Cd were grown with golden luster and uniform composition. These were separated in a Buchner filter and dried in air. The thermogravimetric analysis was performed with a NETZSCH-STA 409 EP Controller.

For the dielectric spectroscopy a pressed pellet of powdered sample, 20 mm in diameter with thickness 0.83 mm was prepared with a pressure pump (Riken Powder model P-1B) at room temperature. Two platinum foil electrodes were pressed at the same time with the sample. The electrical measurements were taken using a low-frequency (0–100 kHz) dynamical signal analyzer (DSA–Hewlett–Packard 3561A) at the temperature range of 240–425 K. The data can be transferred to a PC through an HP 82335 Interface Bus (IEEE-488), where it can be stored and analysed by a software program (*2plt-1996*) [12]. An analytical description of the process is given in previous articles [7,13].

The Raman spectra were obtained at  $4\text{ cm}^{-1}$  resolution from  $3500\text{ cm}^{-1}$  to  $100\text{ cm}^{-1}$  with data point interval of  $1\text{ cm}^{-1}$  using a Perkin–Elmer NIR FT-spectrometer (Spectrum GX II) equipped with an InGaAs detector. The laser power and spot (Nd: YAG at 1064 nm) were controlled to be constant at 50 mW during the measurements and 400 scans were accumulated. Two experiments were performed in the temperature ranges: (a)  $-120$ – $20\text{ }^{\circ}\text{C}$  and (b)  $30$ – $110\text{ }^{\circ}\text{C}$ , with different samples. During the cooling process the sample was enclosed in a glassy tube and held at a constant temperature ( $\pm 1\text{ }^{\circ}\text{C}$ ) by means of a low temperature cell (Ventacon).

The experimental X-ray powder diffraction pattern was obtained with a Siemens D 5000 diffractometer (Cu  $K\alpha 1 = 1.5406\text{ \AA}$ –Cu  $K\alpha 2 = 1.5444\text{ \AA}$  radiation, in  $0.015^{\circ}$  steps, with a dwell time of 10 s/step, scan range:  $5$ – $55^{\circ} 2\theta$ , monochromator: graphite crystal). The calculation of the simulated X-ray powder diffraction pattern of  $(\alpha\text{-CD})_2\cdot\text{Cd}_{0.5}\cdot\text{I}_5\cdot 27\text{H}_2\text{O}$  and the Rietveld refinement were performed by the computer program *Powder-Cell 2.4* developed by G. Nolze and W. Kraus [14].

### 3. Results

#### 3.1. Thermogravimetric analysis

The thermogravimetric analysis (TGA) of  $\alpha$ -Cd complex (Fig. 2) with a heating rate of  $5\text{ }^{\circ}\text{C}/\text{min}$  reveals twenty six water molecules per  $\alpha$ -cyclodextrin dimer, so the general composition is  $(\alpha\text{-CD})_2\cdot\text{Cd}_{0.5}\cdot\text{I}_5\cdot 26\text{H}_2\text{O}$ . The number of the water molecules

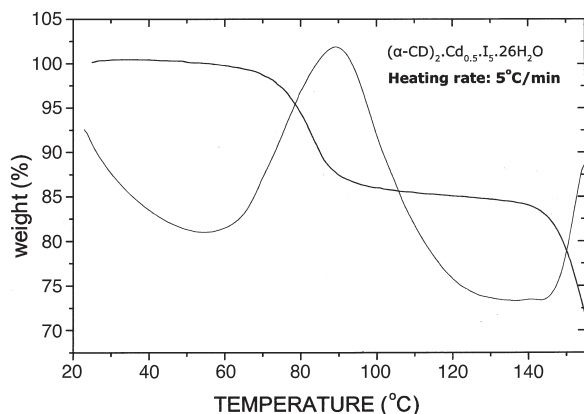


Fig. 2. Simultaneous thermogravimetry (TGA) and differential thermal analysis (DTA) of  $(\alpha\text{-CD})_2\cdot\text{Cd}_{0.5}\cdot\text{I}_5\cdot 26\text{H}_2\text{O}$ .

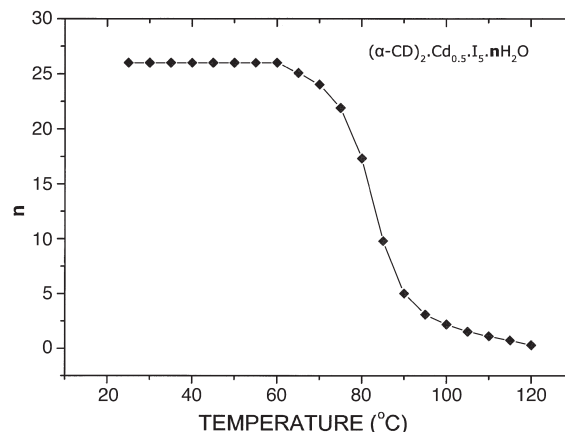


Fig. 3. The variation of the number of water molecules per  $\alpha$ -CD dimer in  $(\alpha\text{-CD})_2\cdot\text{Cd}_{0.5}\cdot\text{I}_5\cdot 26\text{H}_2\text{O}$  during the heating process.

was calculated from the weight loss in the temperature range of  $60$ – $120\text{ }^{\circ}\text{C}$ , where the dehydration process takes place. Fig. 3 shows the number of the remaining water molecules per dimer as the temperature increases.

#### 3.2. X-ray powder diffraction and Rietveld refinement

Few grams of polycrystalline  $(\alpha\text{-CD})_2\cdot\text{Cd}_{0.5}\cdot\text{I}_5\cdot 26\text{H}_2\text{O}$  were finely hand-pulverized in order to reduce the greater volume fraction of certain crystal orientations (texture) in the sample. We collected the experimental XRD pattern at room temperature covering the  $5$ – $55^{\circ} 2\theta$  range, in order to perform a Rietveld refinement. Fig. 4 shows the experimental X-ray powder diffraction pattern. The Rietveld refinement of this profile (*Powder Cell 2.4* software) with the tetragonal  $P4_22_12$  structure of  $(\alpha\text{-CD})_2\cdot\text{Cd}_{0.5}\cdot\text{I}_5\cdot 27\text{H}_2\text{O}$  [2] is also shown in Fig. 4:  $R_p = 6.33\%$ ,  $R_{wp} = 9.17\%$ ,  $R_{exp} = 7.02\%$  and  $\chi^2 = 1.706$ . We obtained a tetragonal  $P4_22_12$  crystal form with the following lattice parameters  $a = b = 19.8460(9)\text{ \AA}$ ,  $c = 30.8593(6)\text{ \AA}$  and  $\alpha = \beta = \gamma = 90.000(0)^{\circ}$  which differ by less than 1% from those values reported by Noltemeyer and Saenger [2]. We note that some experimental peak intensities at room temperature vary from that calculated.

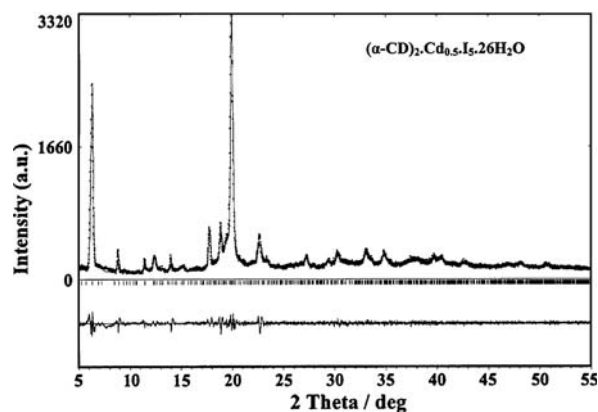


Fig. 4. Rietveld refinement pattern of  $(\alpha\text{-CD})_2\cdot\text{Cd}_{0.5}\cdot\text{I}_5\cdot 26\text{H}_2\text{O}$ . Black circles: experimental pattern, solid line: refined model. The curve at the bottom is the difference between the observed and calculated intensities in the same scale. Black vertical lines indicate the positions of the allowed reflections.

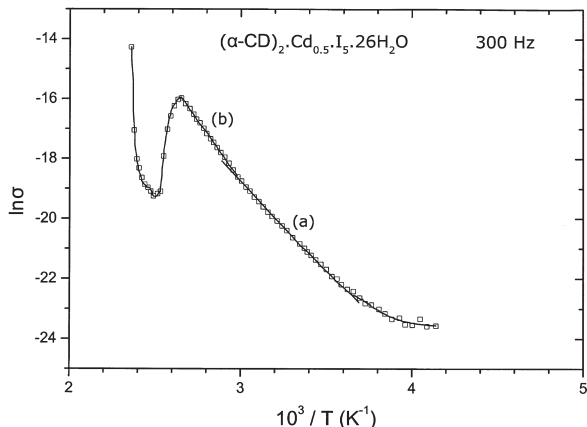


Fig. 5. Temperature dependence of the ac-conductivity ( $\ln\sigma$  vs.  $1/T$ ) of  $(\alpha\text{-CD})_2\cdot\text{Cd}_{0.5}\cdot\text{I}_5\cdot 26\text{H}_2\text{O}$  at 300 Hz.

This is mainly due to the fact that a great percentage of the pentaiodide ions does not follow the  $\text{I}_2\cdot\text{I}^-\cdot\text{I}_2$  geometry which is described by the single crystal X-ray analysis [2]. This becomes evident from the following Raman spectroscopic results. Thus, the different distributions of electronic density result in changes in the theoretical bond lengths and the fractional coordinates of some iodine atoms.

### 3.3. Temperature dependence of the ac-conductivity and the phase shift

The temperature dependence of the ac-conductivity ( $\ln\sigma$  vs.  $1/T$ ) and the phase shift over the range of 240–425 K at frequency 300 Hz is shown in Figs. 5, 6 for  $(\alpha\text{-CD})_2\cdot\text{Cd}_{0.5}\cdot\text{I}_5\cdot 26\text{H}_2\text{O}$ .

The ac-conductivity takes very low values at  $10^3/T > 3.62 \text{ K}^{-1}$  ( $T < 276.2 \text{ K}$ ) and presents two linear parts (a), (b) in the temperature ranges  $2.98 \text{ K}^{-1} < 10^3/T < 3.62 \text{ K}^{-1}$  ( $276.2 \text{ K} < T < 335.6 \text{ K}$ ) and  $2.65 \text{ K}^{-1} < 10^3/T < 2.98 \text{ K}^{-1}$  ( $335.6 \text{ K} < T < 377.0 \text{ K}$ ), respectively. At  $10^3/T < 2.65 \text{ K}^{-1}$  ( $T > 377.0 \text{ K}$ ) it decreases rapidly up to  $10^3/T = 2.49 \text{ K}^{-1}$  ( $T = 401.6 \text{ K}$ ) and then increases to a topical maximum at  $10^3/T = 2.46 \text{ K}^{-1}$  ( $T = 406.5 \text{ K}$ ). Finally, at  $10^3/T < 2.42 \text{ K}^{-1}$  ( $T > 413.2 \text{ K}$ ) the ac-conductivity increases abruptly up to  $10^3/T = 2.36 \text{ K}^{-1}$  ( $T = 424.1 \text{ K}$ ).

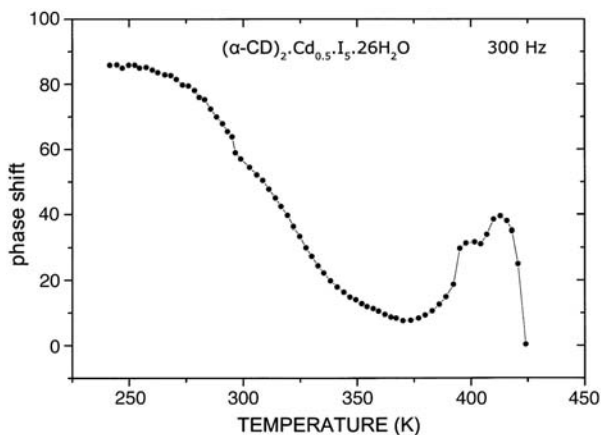


Fig. 6. Temperature dependence of the phase shift of  $(\alpha\text{-CD})_2\cdot\text{Cd}_{0.5}\cdot\text{I}_5\cdot 26\text{H}_2\text{O}$  at 300 Hz.

The phase shift drops gradually from the value  $85.8^\circ$  at 241.5 K to a minimum value  $7.7^\circ$  at 373.5 K, then it increases to a double peak with maximum values  $31.7^\circ$  at 401.6 K and  $39.5^\circ$  at 412.9 K and minimum value  $31.1^\circ$  at 404.3 K. Finally, at  $T > 412.9 \text{ K}$ , it drops rapidly to the value  $0.4^\circ$  at 424.1 K.

### 3.4. Impedance plots

The impedance plot  $\text{Im}Z$  vs.  $\text{Re}Z$  (0–100 kHz) of  $\alpha\text{-Cd}$  in the temperature range of 293.1–314.1 K (Fig. 7A) shows circular

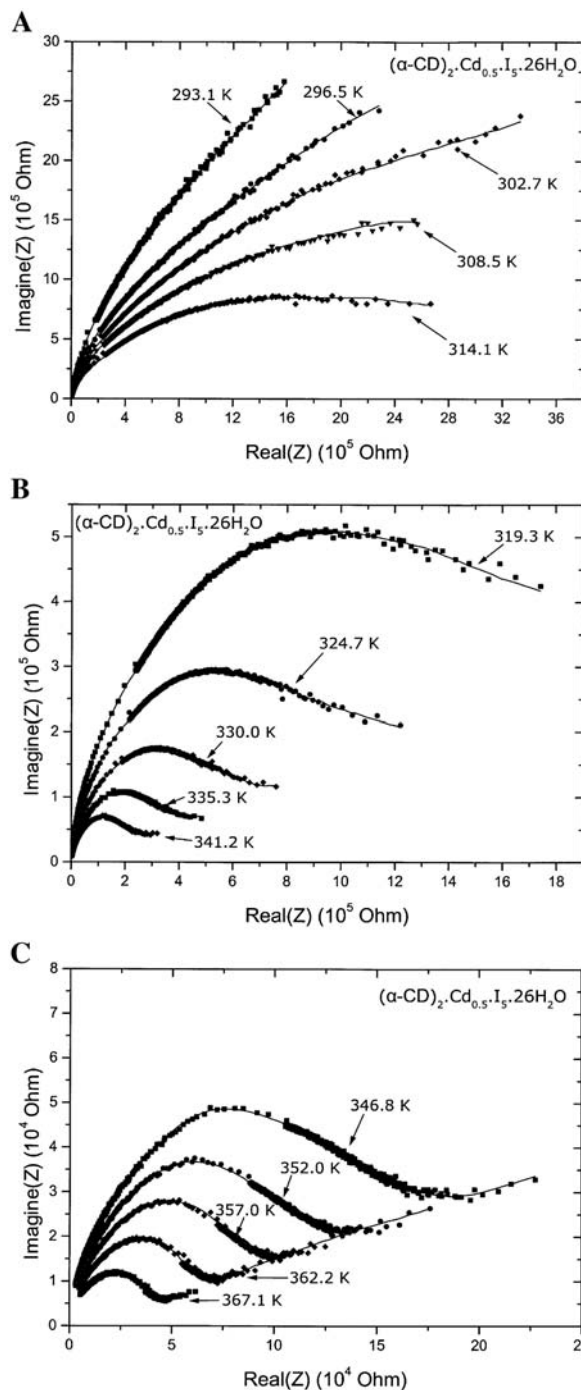


Fig. 7. Impedance plot of  $(\alpha\text{-CD})_2\cdot\text{Cd}_{0.5}\cdot\text{I}_5\cdot 26\text{H}_2\text{O}$  in the temperature range of: (A) 293.1–314.1 K, (B) 319.3–341.2 K and (C) 346.8–367.1 K.



arcs of gradually decreased radius as the temperature increases. In the temperature range of 319.3–341.2 K (Fig. 7B) the plot shows nearly semicircular arcs of gradually decreased radius. At approximately  $T > 333$  K a linear segment is generated at low frequencies. Finally, in the range of 346.8–367.1 K (Fig. 7C) there are depressed semicircles with well-distinguished linear responses in the low frequency region.

### 3.5. Raman spectra

The Raman spectra of  $\alpha$ -Cd during the cooling process are shown in Fig. 8A, for the different temperatures 20, 0, –20, –40, –60, –80, –120 °C. Initially at 20 °C there is a strong peak at 160  $\text{cm}^{-1}$  with intensity 47.92 and a shoulder at 168  $\text{cm}^{-1}$  with intensity 31.31. From 0 to –120 °C the intensity of the band at 160  $\text{cm}^{-1}$  increases while the shoulder at 168  $\text{cm}^{-1}$  gradually disappears. The Raman spectra during the heating process are shown in Fig. 8B, for the different temperatures 30, 50, 70, 90, 110 °C. At 30 °C a double broad band appears with maximum intensity 49.89. In the range of 50–110 °C there is only one band at 168  $\text{cm}^{-1}$  with gradually

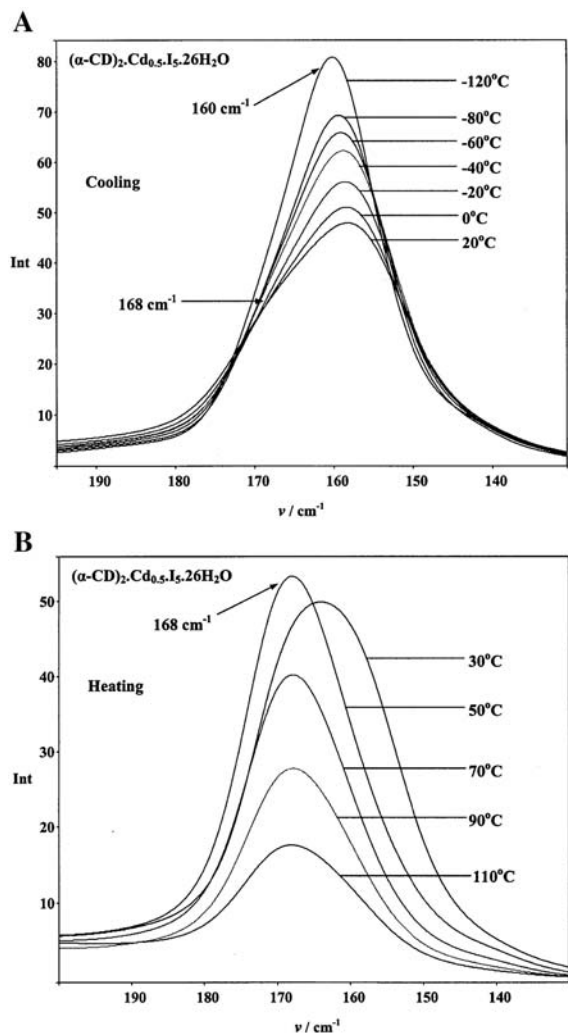


Fig. 8. Raman spectra of  $(\alpha\text{-CD})_2\cdot\text{Cd}_{0.5}\cdot\text{I}_5\cdot 26\text{H}_2\text{O}$  in the temperature range of: (A) –120–20 °C (cooling) and (B) 30–110 °C (heating).

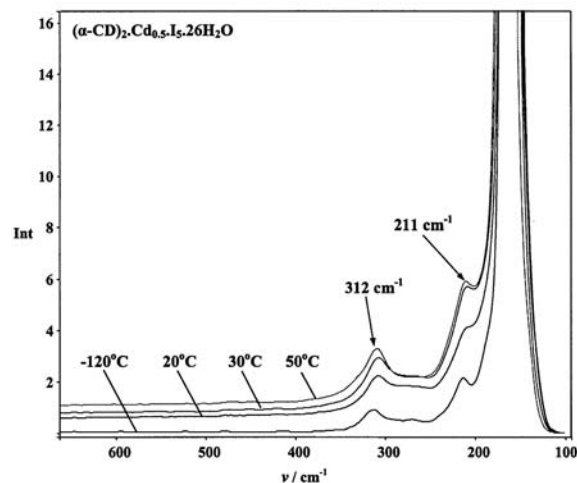


Fig. 9. Raman overtones of  $(\alpha\text{-CD})_2\cdot\text{Cd}_{0.5}\cdot\text{I}_5\cdot 26\text{H}_2\text{O}$  at the representative temperatures: (a) 20, –120 °C (cooling) and (b) 30, 50 °C (heating).

decreased intensity. Fig. 9 shows the Raman spectra at the representative temperatures 20, –120 °C and 30, 50 °C in the extended frequency range of 100–650  $\text{cm}^{-1}$ . Two more bands are observed at 211  $\text{cm}^{-1}$  and at 312  $\text{cm}^{-1}$  whose intensity decreases during cooling and increases during heating.

## 4. Discussion



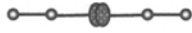




The negligible values of the ac-conductivity at  $T < 276.2$  K (Fig. 5) indicate that most of the water molecules remain tightly bound. At  $T > 276.2$  K the ac-conductivity increases linearly according to the Arrhenius equation  $\sigma = \sigma_0 \exp(-E_W/2k_B T)$  with activation energy  $E_a = 0.51$  eV in the temperature range of 276.2–335.6 K (linear part (a)) and  $E_a = 0.67$  eV in the range of 335.6–377.0 K (linear part (b)). This behaviour is a resultant of the following mechanisms:

- The continuous transformation of the tightly bound water molecules to easily movable:  $(\text{H}_2\text{O})_{\text{tightlybound}} \rightarrow (\text{H}_2\text{O})_{\text{easily movable}}$ .
- The contribution of the metallic ions via the water-net.
- The gradual removal of the easily movable water molecules.

As it becomes evident from the TGA curve of  $\alpha$ -Cd (Fig. 2), the easily movable water molecules start to escape at approximately 333 K (60 °C). Despite this progressive dehydration process the slope of the above Arrhenius increment does not decrease (lower increasing rate) until 377.0 K due to the fact that the components (a) and (b) counterbalance the gradual breakdown of the water-net. This is clearly indicated in the impedance plots (Fig. 7A, B) where the continuously decreased radius of the arcs as the temperature increases, indicates the continuous transformation (a). The linear responses in the low frequency region (Fig. 7B, C) reveal the onset of space charge which is directly related to the metallic ions' movements (b) [8,15,16]. Initially, the disordered metallic ions are restricted and make no contribution to the ac-

Table 1

The coexistence of the two pentaiodide forms  $I_2 \cdot \Gamma \cdot I_2$ ,  $I_3 \cdot I_2 \leftrightarrow I_2 \cdot I_3$  at 20 °C and the progressive variation of the occupancy ratio of  $\Gamma$  ions as the temperature decreases up to -120 °C

Temperature	Cooling process	
	Transformations of the pentaiodides (x/y): the occupancy ratio of the central $\Gamma$ ion	
20 °C	$I_2 \cdot \Gamma \cdot I_2$ (50/50) 	$\Gamma_3 \cdot I_2 \leftrightarrow I_2 \cdot \Gamma_3$ (e.g. ...60/40...70/30...) 
-60 °C	$I_2 \cdot \Gamma \cdot I_2$ (50/50) 	$\Gamma_3 \cdot I_2 \leftrightarrow I_2 \cdot \Gamma_3$ (e.g. ...55/45...65/35...)  and $I_2 \cdot \Gamma \cdot I_2$ (50/50) 
-120 °C	$I_2 \cdot \Gamma \cdot I_2$ (50/50) 	$I_2 \cdot \Gamma \cdot I_2$ (50/50) 

conductivity since the surrounding water molecules remain tightly bound. At approximately 333 K (60 °C) – where the dehydration process begins – the cadmium ions are released and start to oscillate with the frequency of the applied alternating field. Their contribution is facilitated by their hydration shells via a chemical exchange of  $H^+$  between the water molecules, described as Grotthuss mechanism [17–19]. This procedure justifies the greater activation energy of the linear part (b) compared to that of the linear part (a) in the  $\ln\sigma$  vs.  $1/T$  plot. In the temperature range of 377.0–401.6 K, the ac-conductivity drops rapidly to a minimum value because the water-net includes very few water molecules ( $\sim 2.5$  molecules per dimer according to Fig. 3) and the already depleted metallic ions act as localized charges.

In the  $\varphi$  vs.  $T$  plot (Fig. 6) the rapid decrease of the phase shift to a minimum value at  $T=373.5$  K is a result of the exponential increment of the ac-conductivity. The following rise of  $\varphi$  at  $373.5 < T < 401.6$  K is caused by the rapid decrease of the ac-conductivity in the same range. At  $T=404.3$  K the topical minimum of  $\varphi$  is exclusively attributed to a transformation of the pentaiodide ions whereas the abrupt decrease at  $T > 412.9$  K is due to the sublimation of iodine. This is elucidated by the Raman spectroscopic results.












At room temperature (20 °C) the initial Raman bands at 160 and 168  $cm^{-1}$  indicate the coexistence of two kinds of pentaiodide units ( $I_2 \cdot \Gamma \cdot I_2$ ,  $I_3 \cdot I_2$ ) in the polyiodide chains. The former band is ascribed to the symmetric stretch of the outer I–I bonds of the  $I_2 \cdot \Gamma \cdot I_2$  anions [11,20–23], whereas the latter one to a weakly coordinated  $I_2$  molecule in a  $I_3 \cdot I_2$  pentaiodide [24]. In the case of the  $I_2 \cdot \Gamma \cdot I_2$  units the central iodine ion  $\Gamma$  is expected to be twofold disordered at 50/50 occupancy [2]. When the central  $\Gamma$  ion presents occupancy ratio different from 50/50 (e.g. ...60/40...70/30...) the pentaiodide unit takes a

$I_3 \cdot I_2 \leftrightarrow I_2 \cdot I_3$  form, as in the case of  $(\alpha\text{-CD})_2 \cdot LiI_3 \cdot I_2 \cdot 8H_2O$  where the  $\alpha\text{-CD}$  dimer accommodates two units  $I_3 \cdot I_2$  or  $I_2 \cdot I_3$  in the statistical occupancy ratio 69/31 [2]. During the cooling process the shoulder at 168  $cm^{-1}$  disappears showing the transformation of the initial  $I_3 \cdot I_2 \leftrightarrow I_2 \cdot I_3$  units to  $I_2 \cdot \Gamma \cdot I_2$  type. As the temperature decreases the occupancy ratio of the central  $\Gamma$  ion in these  $I_3 \cdot I_2 \leftrightarrow I_2 \cdot I_3$  units gradually changes, having the tendency to take the value 50/50. The occupancy ratio 50/50 of the initial (20 °C)  $I_2 \cdot \Gamma \cdot I_2$  units remains constant (Table 1).

On the contrary, in the heating process the band at 160  $cm^{-1}$  disappears and at 50 °C there is only one strong band at 168  $cm^{-1}$  indicating the transformation of the initial  $I_2 \cdot \Gamma \cdot I_2$  units to  $I_3 \cdot I_2 \leftrightarrow I_2 \cdot I_3$  type. This transformation is due to the changes of the occupancy ratio of the  $\Gamma$  ions (50/50  $\rightarrow$  ...55/45...60/40...). Similar changes also happen to the occupancy ratio of the  $\Gamma$  ions in the initial (20 °C)  $I_3 \cdot I_2 \leftrightarrow I_2 \cdot I_3$  units (e.g. ...60/40...70/30...  $\rightarrow$  ...65/35...75/25...) (Table 2). Therefore, it appears to be explicit that as the temperature increases the occupancy ratio of the disordered  $\Gamma$  ions in all the pentaiodide units of the sample continuously changes having the tendency to take the value 100/0 (full occupancy). When such an order–disorder transition ( $I_3 \cdot I_2 \leftrightarrow I_2 \cdot I_3 \rightarrow$

Table 2

The coexistence of the two pentaiodide forms  $I_2 \cdot \Gamma \cdot I_2$ ,  $I_3 \cdot I_2 \leftrightarrow I_2 \cdot I_3$  at 20 °C and the progressive variation of the occupancy ratio of  $\Gamma$  ions as the temperature increases up to 130 °C

Temperature	Heating process	
	Transformations of the pentaiodides (x/y): the occupancy ratio of the central $\Gamma$ ion	
20 °C	$I_2 \cdot \Gamma \cdot I_2$ (50/50) 	$\Gamma_3 \cdot I_2 \leftrightarrow I_2 \cdot \Gamma_3$ (e.g. ...60/40...70/30...) 
50 °C	$\Gamma_3 \cdot I_2 \leftrightarrow I_2 \cdot \Gamma_3$ (e.g. 55/45) 	$\Gamma_3 \cdot I_2 \leftrightarrow I_2 \cdot \Gamma_3$ (e.g. ...65/35...75/25...) 
80 °C	$\Gamma_3 \cdot I_2 \leftrightarrow I_2 \cdot \Gamma_3$ (e.g. 60/40) 	$\Gamma_3 \cdot I_2 \leftrightarrow I_2 \cdot \Gamma_3$ (e.g. ...70/30...80/20...) 
110 °C	$\Gamma_3 \cdot I_2 \leftrightarrow I_2 \cdot \Gamma_3$ (e.g. 65/35) 	$\Gamma_3 \cdot I_2 \leftrightarrow I_2 \cdot \Gamma_3$ (e.g. ...75/25...85/15...) 
130 °C	$\Gamma_3 \cdot I_2 \leftrightarrow I_2 \cdot \Gamma_3$ (e.g. 70/30) 	$\Gamma_3 \cdot I_2 \leftrightarrow I_2 \cdot \Gamma_3$ (e.g. ...80/20...90/10...)  and $\Gamma_3 \cdot I_2$ (100/0) 

$I_3 \cdot I_2$ ) takes place in some  $I_5$  units, the charge transfer between the  $I^-$  ion (Lewis base donor) and one of the two  $I_2$  molecules (Lewis acid acceptor) [24] results in the drop of  $\varphi$  to the topical minimum at 404.3 K (Fig. 6). The other iodine molecule  $I_2$  of these pentaiodides becomes very weakly coordinated.

The above topical minimum value of the phase shift is followed by an abrupt decrease at  $T > 412.9$  K due to the sublimation of  $I_2$  molecules, which shortens the neighboring  $I_5$  units providing conductive paths [25] along the polyiodide chains. This is also confirmed by the great weight loss of the TGA curve at approximately 140 °C (413 K) (Fig. 2). The temperature ( $\sim 140$  °C) at which the sublimation of iodine takes place in  $\alpha$ -Cd complex is higher than that in the case of  $\beta$ -Ba,  $\beta$ -Cd,  $\beta$ -Li,  $\beta$ -K and  $\beta$ -Cs complexes ( $\sim 130$  °C) [7–9]. That happens because the neighboring pentaiodide ions  $I_5^-$  of  $\alpha$ -Cd are weakly interactive whereas the heptaiodide ions  $I_7^-$  in the  $\beta$ -CD complexes are non interactive. Similar results have been obtained for the  $\alpha$ -CD pentaiodide complexes with sodium and barium metals [26].

The  $I_3^-$  ions have a characteristic Raman-active (symmetric stretch) band  $\nu_1$  at 105–110  $\text{cm}^{-1}$  [11,20–24]. The Raman spectroscopy study of the  $I_3^-$  chain compound (benzamide)<sub>2</sub>- $H^+I_3^-$  by Teitelbaum et al. [20] showed a strong band at 108  $\text{cm}^{-1}$  ( $\nu_1$ ) and two progressive overtones. Additionally, the Raman investigation of  $\alpha$ -Cd by Mizuno et al. [11] at room temperature, showed a main band at 161  $\text{cm}^{-1}$  ( $I_5^-$ ) and a second band at 107  $\text{cm}^{-1}$  which was attributed to  $I_3^-$  impurities. In our case, we did not observe the band at 107  $\text{cm}^{-1}$  corresponding to the  $I_3^-$  ions of the  $I_3 \cdot I_2 \leftrightarrow I_2 \cdot I_3$  form, because of the limited frequency range of the spectrometer. Instead of this, we associate the observed overtones at 211  $\text{cm}^{-1}$  ( $2 \times 107$ ) and at 312  $\text{cm}^{-1}$  ( $3 \times 107$ ) with the existence of  $I_3^-$  ions in the pentaiodide units. Their intensity decreases during the cooling process due to the gradual transformation ( $I_3 \cdot I_2 \leftrightarrow I_2 \cdot I_3$ )  $\rightarrow$  ( $I_2 \cdot I^- \cdot I_2$ ) and increases during heating because of the inverse transformation ( $I_2 \cdot I^- \cdot I_2$ )  $\rightarrow$  ( $I_3 \cdot I_2 \leftrightarrow I_2 \cdot I_3$ ).

## 5. Conclusions

Two kinds of pentaiodide units  $I_2 \cdot I^- \cdot I_2$  and  $I_3 \cdot I_2 \leftrightarrow I_2 \cdot I_3$  coexist in the polyiodide chain of  $(\alpha\text{-CD})_2 \cdot \text{Cd}_{0.5} \cdot I_5 \cdot 26\text{H}_2\text{O}$  at room temperature, as it is indicated by the characteristic Raman bands at 160 and 168  $\text{cm}^{-1}$ , respectively. The central  $I^-$  ion is disordered in occupancy ratio 50/50 in the  $I_2 \cdot I^- \cdot I_2$  type and different from 50/50 (e.g. ...60/40...70/30...) in the case of the  $I_3 \cdot I_2 \leftrightarrow I_2 \cdot I_3$  type.

At low temperatures the transformation ( $I_3 \cdot I_2 \leftrightarrow I_2 \cdot I_3$ )  $\rightarrow$  ( $I_2 \cdot I^- \cdot I_2$ ) takes place, whereas at high temperatures the inverse one ( $I_2 \cdot I^- \cdot I_2$ )  $\rightarrow$  ( $I_3 \cdot I_2 \leftrightarrow I_2 \cdot I_3$ ) happens. During the heating process the topical minimum of the phase shift at 404.3 K reveals an order–disorder transition, since in some of the pentaiodide

units  $I_3 \cdot I_2 \leftrightarrow I_2 \cdot I_3$  the disordered  $I^-$  ion becomes well-ordered (full occupancy 100/0).

The Arrhenius exponential behaviour of the ac-conductivity in the temperature range 276.2 K  $< T < 377.0$  K is not affected by the dehydration process which starts at approximately 333 K, because of the continuous transformation  $(\text{H}_2\text{O})_{\text{tightlybound}} \rightarrow (\text{H}_2\text{O})_{\text{easilymovable}}$  and the contribution of the metallic ions via the water-net. When most of the water molecules have been removed from the lattice, the already depleted metallic ions act as localized charges making no longer a contribution to the ac-conductivity.

Finally, the abrupt increase of the ac-conductivity at  $T > 413.2$  K is caused by the sublimation of iodine which provides conductive paths along the polyiodide chains.

## Acknowledgments

This work was partly supported by Grant No. 70/4/3347SARG, NKUA. We thank Prof. K. Viras for his assistance in the Raman Spectra.

## References

- [1] C. Betzel, B. Hingerty, M. Noltemeyer, G. Weber, W. Saenger, J.A. Hamilton, *J. Incl. Phenom.* 1 (1983) 181.
- [2] M. Noltemeyer, W. Saenger, *J. Am. Chem. Soc.* 102 (1980) 2710.
- [3] M. Noltemeyer, W. Saenger, *Nature* 259 (1976) 629.
- [4] T.C. Ghikas, J.C. Papaioannou, *Mol. Phys.* 100 (2002) 673.
- [5] C. Betzel, W. Saenger, B.E. Hingerty, G.M. Brown, *J. Am. Chem. Soc.* 106 (1984) 7545.
- [6] V. Zabel, W. Saenger, S.A. Mason, *J. Am. Chem. Soc.* 108 (1986) 3664.
- [7] V.G. Charalampopoulos, J.C. Papaioannou, *Mol. Phys.* 103 (2005) 2621.
- [8] J.C. Papaioannou, V.G. Charalampopoulos, P. Xynogalas, K. Viras, *J. Phys. Chem. Solids* 67 (2006) 1379.
- [9] V.G. Charalampopoulos, J.C. Papaioannou, H.S. Karayianni, *Solid State Sciences* 8 (2006) 97.
- [10] J.C. Papaioannou, T.C. Ghikas, *Mol. Phys.* 101 (2003) 2601.
- [11] M. Mizuno, J. Tanaka, I. Harada, *J. Phys. Chem.* 85 (1981) 1789.
- [12] K. Tampouris, J.C. Papaioannou, (unpublished results).
- [13] J.C. Papaioannou, N. Papadimitropoulos, I. Mavridis, *Mol. Phys.* 97 (1999) 611.
- [14] G. Nolze, W. Kraus, *Powder Diffr.* 13 (1998) 256.
- [15] A.K. Jonscher, *J. Mater. Sci.* 13 (1978) 553.
- [16] J.R. Macdonald, *Impedance Spectroscopy*, Wiley, New York, 1987, p. 252.
- [17] N. Agmon, *Chem. Phys. Lett.* 244 (1995) 456.
- [18] B.V. Merinov, *Solid State Ionics* 84 (1996) 89.
- [19] R. Pomes, B. Roux, *Biophys. J.* 82 (2002) 2304.
- [20] R.C. Teitelbaum, S.L. Ruby, T.J. Marks, *J. Am. Chem. Soc.* 102 (1980) 3322.
- [21] E.M. Nour, L.H. Chen, J. Laane, *J. Phys. Chem.* 90 (1986) 2841.
- [22] X. Yu, C. Houtman, R.H. Atalla, *Carbohydr. Res.* 292 (1996) 129.
- [23] X. Yu, R.H. Atalla, *Carbohydr. Res.* 340 (2005) 981.
- [24] P.H. Svensson, L. Kloo, *Chem. Rev.* 103 (2003) 1649.
- [25] A. Oza, *Cryst. Res. Technol.* 19 (1984) 697.
- [26] V.G. Charalampopoulos, J.C. Papaioannou, (in preparation).